

TABLE 1 Anisotropy of Natural Pine Wood and Pressed Wood Samples

Sample	Pressed	Pine1	Pine2
d (mm)	9.90	8.50	15.3
α_{\max} (°)	0.79	11.8	31.2
δ (°)	0.001	39.9	70.8
ψ (°)	44.5	37.5	32.8
$\Delta n'$	0.000	0.130	0.129
$\Delta n''$	0.003	0.050	0.046

about the same as these two samples were taken from the same piece of wood.

5. CONCLUSIONS

In this article, we have presented the principles of a microwave polarimetric method to determine natural or inferred anisotropy of materials. We have studied its feasibility with wood samples, and results were close to those attempted. The applications of this method can be extended to a wide range of nontransparent materials such as extruded plastic, leather, etc. Such a contactless bench is of great interest for manufacturing industries and can be optimized for mobile using.

REFERENCES

1. A.M. Nicolson and G.F. Ross, Measurement of the intrinsic properties of materials by time-domain techniques, *IEEE Trans Instrum Meas* 19 (1970), 377–382.
2. S. Biju Kumar, U. Raveendranath, P. Mohanan, K.T. Mathew, M. Hajian, and L.P. Ligthart, A simple free-space method for measuring the complex permittivity of single and compound dielectric materials, *Microwave Opt Technol Lett* 26 (2000), 117–119.
3. F. Sagnard, D. Seetharamdoo, and V.L. Glaunec, Reflection and transmission ellipsometry data analysis for measuring the complex permittivity of a single-layer material at microwave frequencies, *Microwave Opt Technol Lett* 33 (2002), 443–448.
4. F. Sagnard, F. Bentabet, and C. Vignat, In situ measurements of the complex permittivity of materials using reflection ellipsometry in the microwave band: Theory (part I). *IEEE Trans Instrum Meas* 54 (2005), 1266–1273.
5. F. Sagnard, F. Bentabet, and C. Vignat, In situ measurements of the complex permittivity of materials using reflection ellipsometry in the microwave band: Experiments (part II). *IEEE Trans Instrum Meas* 54 (2005), 1274–1282.
6. G. Raoult, *Les ondes centimétriques*, Masson, Paris, 1958.
7. R.M.A. Azzam and N.M. Bashara, *Ellipsometry and polarized light*, Elsevier science, Amsterdam, 1987.

© 2011 Wiley Periodicals, Inc.

SMALL-SIZE WIDEBAND CHIP ANTENNA FOR WWAN/LTE OPERATION AND CLOSE INTEGRATION WITH NEARBY CONDUCTING ELEMENTS IN THE MOBILE HANDSET

Shu-Chuan Chen and Kin-Lu Wong

Department of Electrical Engineering, National Sun Yat-sen University, Kaohsiung 80424, Taiwan; Corresponding author: wongkl@ema.ee.nsysu.edu.tw

Received 1 December 2010

ABSTRACT: A wideband chip antenna having a small size of $3 \times 15 \times 35 \text{ mm}^3$ for application in the mobile handset to cover eight-band

WWAN/LTE operation is presented. The antenna is mainly formed by a direct-feed two-branch strip and a coupled-fed shorted strip. The two-branch strip functions as an efficient radiator and also as a coupling feed to capacitively excite the shorted strip. The coupled-fed shorted strip contributes a wide resonant mode at about 800 MHz to cover the LTE700/GSM850/900 (704~960 MHz) operation. The two-branch strip and the shorted strip together contribute their fundamental or higher-order resonant modes to cover the GSM1800/1900/UMTS/LTE2300/2500 (1710~2690 MHz) operation. There are also ground planes located on two side surfaces of the chip antenna, which are grounded to the system ground plane printed on the main circuit board of the mobile handset. This configuration allows the antenna to be closely integrated with nearby conducting or electronic elements such as a universal series bus connector to achieve compact integration of the internal antenna in the mobile handset. Details of the proposed antenna are presented. © 2011 Wiley Periodicals, Inc. *Microwave Opt Technol Lett* 53:1998–2004, 2011; View this article online at wileyonlinelibrary.com. DOI 10.1002/mop.26200

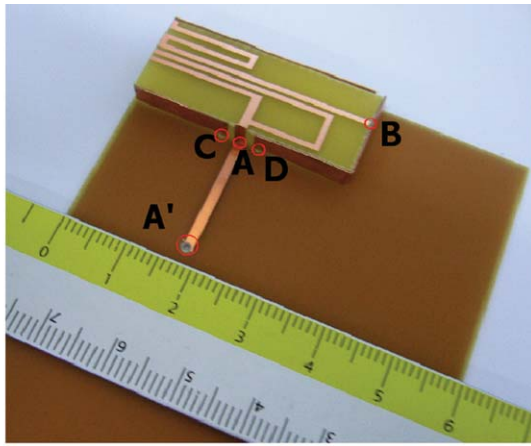
Key words: mobile antennas; internal handset antennas; LTE antennas; WWAN antennas; chip antennas

1. INTRODUCTION

Owing to the perspective long-term evolution (LTE) operation for providing better mobile broadband and multimedia services than the wireless wide area network (WWAN) systems, the eight-band internal WWAN/LTE antenna for modern mobile handsets is hence demanded, and some promising WWAN/LTE internal handset antennas have also been reported recently [1–8]. Most of these promising antennas [1–6] are mainly to be directly printed on the main circuit board of the mobile handset. Surface-mount-type chip antennas for WWAN/LTE operation have also been shown [7, 8]. These antennas, similar to many traditional internal WWAN handset antennas [9–16], are required to have a certain isolation distance to the nearby conducting elements such as the system ground plane printed on the main circuit board or the universal series bus (USB) connector located at the bottom edge of the main circuit board [17, 18]. This characteristic limits the compact integration of the internal WWAN/LTE antennas inside the mobile handset.

In this article, we report a promising internal WWAN/LTE antenna that has the advantages of small size, wideband operation and capable of close integration with nearby conducting elements inside the mobile handset. The proposed antenna covers eight-band WWAN/LTE operation and has a size of $3 \times 15 \times 35 \text{ mm}^3$ only. The antenna can generate two wide operating bands to cover the LTE700/GSM850/900 operation in the 704~960 MHz band and the GSM1800/1900/UMTS/LTE2300/2500 operation in the 1710~2690 MHz band. The antenna mainly consists of a direct-feed two-branch strip and a coupled-fed shorted strip. The latter is capacitively excited by the two-branch strip, and its front end is short-circuited to the ground planes located on two side surfaces of the chip antenna.

In practical applications, the chip antenna is to be surface-mounted onto one of the corners of the main circuit board (see Fig. 1 for example), with the antenna's ground planes on its two side surfaces grounded to the system ground plane on the main circuit board of the mobile handset. In this case, the antenna's side ground planes can serve as shielding walls to suppress the possible fringing electromagnetic fields of the antenna [19–23] such that small or neglecting coupling effects between the antenna and nearby electronic or conducting elements on the main circuit board of the mobile handset can be obtained. This behavior can lead to very close integration of the proposed internal WWAN/LTE chip antenna inside the mobile handset. Details



AA': 50-Ω feedline for testing the antenna in the experiment
A': via-hole to a 50-Ω SMA connector on back side of the experiment

Figure 2 Photos of the fabricated antenna mounted on the main circuit board; the plastic housing not shown. [Color figure can be viewed in the online issue, which is available at wileyonlinelibrary.com]

(704 ~ 960 MHz) and upper band (1710 ~ 2690 MHz) are better than 3:1 VSWR or 6-dB return loss, which is generally used as the design specification for practical internal handset antenna applications.

To analyze the antenna's operating principle, Figure 4 shows the simulated return loss for the proposed antenna, the case with Strip 1 only (denoted as R1), and the case with Strips 1 and 2 or the two-branch strip only (denoted as R2). For R1, two resonant modes at about 1.5 and 2.9 GHz are excited, with the 1.5-GHz mode being the quarter-wavelength resonant mode related to Strip 1 and the 2.9-GHz mode being the higher-order resonant mode. When Strip 2 is added to form R2, an additional resonant mode occurred at about 2.2 GHz is seen, although the impedance matching is not better than 6-dB return loss. For R2, it is also noted that the two resonant modes contributed by Strip 1 are shifted owing to the coupling effects between Strips 2 and 1. Finally, by adding Strip 3 to form the proposed antenna, a dual-resonance quarter-wavelength mode at about 800 MHz is generated, which covers the desired 704~ 960 MHz band. In addition, two higher-order resonant modes at about 1.7 and 3.1 GHz

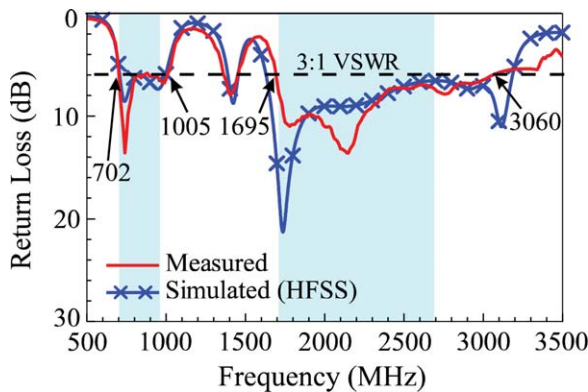


Figure 3 Measured and simulated return loss for the fabricated antenna. [Color figure can be viewed in the online issue, which is available at wileyonlinelibrary.com]

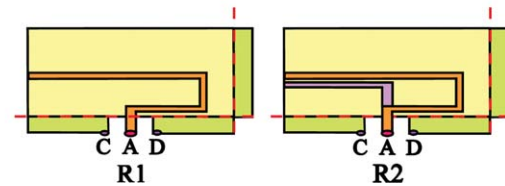
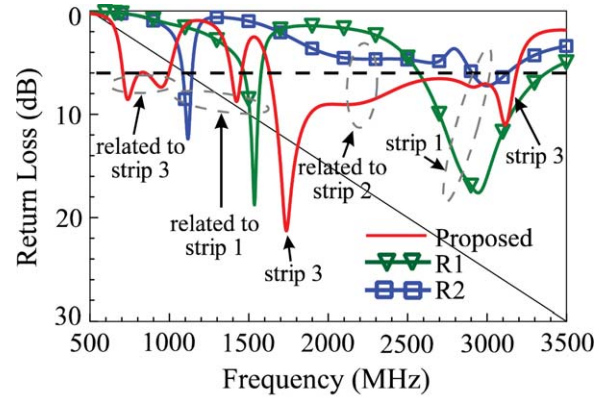


Figure 4 Simulated return loss for the proposed antenna, the case with strip 1 only (R1), and the case with Strips 1 and 2 only (R2). [Color figure can be viewed in the online issue, which is available at wileyonlinelibrary.com]

are generated to combine with the resonant modes contributed by Strips 1 and 2 to form a wide upper band for the antenna to cover the desired 1710 ~ 2690 MHz band.

Figure 5 shows the simulated return loss as a function of the coupling gap g between Strips 1 and 3. Other dimensions are the same as in Figure 1. Results for the coupling gap g varied from 0.2 to 0.8 mm are presented. Large effects on the impedance matching for frequencies over the lower band are seen. Results indicate that a proper width g of the coupling gap is important in achieving good impedance matching over the desired lower band of 704 ~ 960 MHz. The preferred coupling gap g is 0.5 mm in the proposed antenna. For frequencies over the desired upper band, the coupling gap g shows relatively small effects on the impedance matching.

Figure 6 shows the simulated return loss as a function of the distance d between strip 1 and 2, and other dimensions are the same as in Figure 1. Effects of the distance d on the impedance

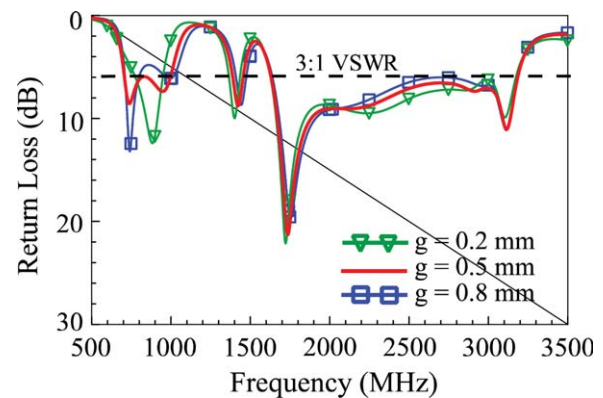


Figure 5 Simulated return loss as a function of the coupling gap g between Strips 1 and 3. Other dimensions are the same as in Figure 1. [Color figure can be viewed in the online issue, which is available at wileyonlinelibrary.com]

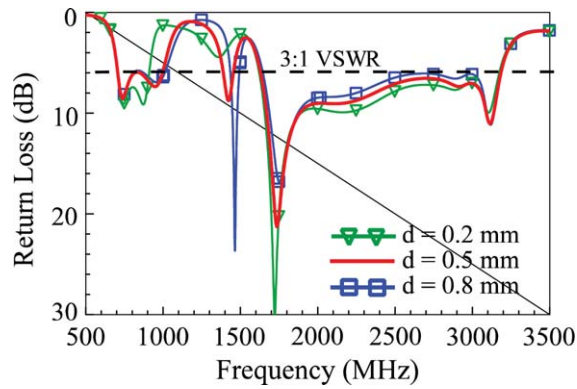
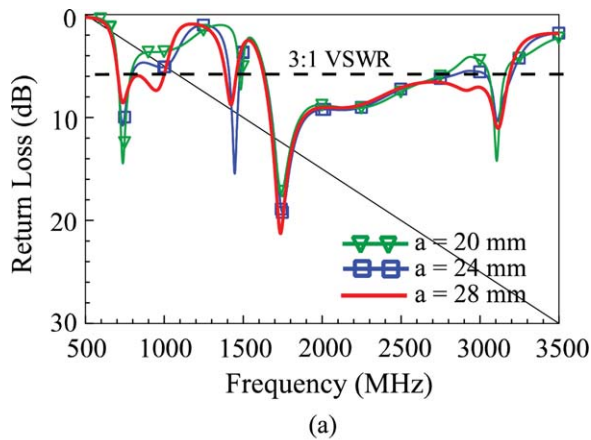


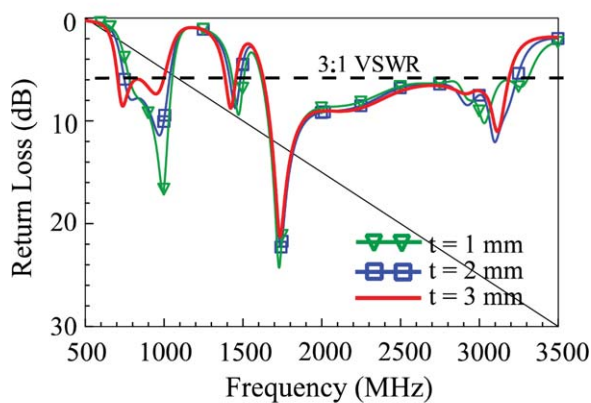
Figure 6 Simulated return loss as a function of the distance d between Strips 1 and 2. Other dimensions are the same as in Figure 1. [Color figure can be viewed in the online issue, which is available at wileyonlinelibrary.com]

matching of the antenna are seen to be similar to those of the coupling gap g shown in Figure 5. A proper distance d between Strips 1 and 2 is also important in achieving a wide lower band to cover the desired 704 ~ 960 MHz band.

Effects of the end-section length a of Strip 1 and the end-section width t of Strip 3 are also studied. Results for the length a varied from 20 to 28 mm are presented in Figure 7(a),



(a)



(b)

Figure 7 Simulated return loss as a function of (a) the end-section length a of Strip 1 and (b) the end-section width t of Strip 3. Other dimensions are the same as in Figure 1. [Color figure can be viewed in the online issue, which is available at wileyonlinelibrary.com]

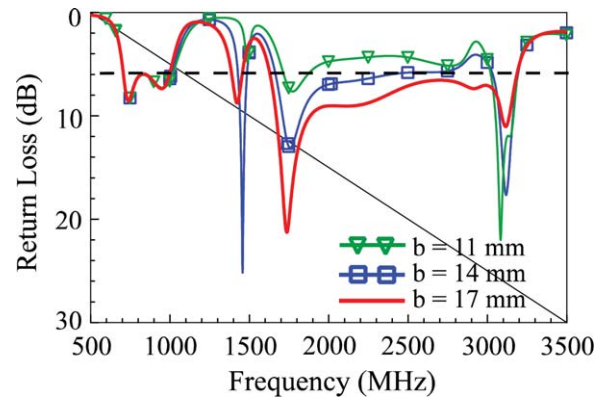


Figure 8 Simulated return loss as a function of the end-section length b of Strip 2. Other dimensions are the same as in Figure 1. [Color figure can be viewed in the online issue, which is available at wileyonlinelibrary.com]

whereas those for the width t varied from 1 to 3 mm are shown in Figure 7(b). As the variation in the length a will cause strong effects on the capacitive coupling between the two-branch strip and Strip 3, the excitation of the dual-resonance quarter-wavelength mode of Strip 3 is greatly affected as seen in Figure 7(a). For the variation in the width t , it causes some shifting in the excited dual-resonance quarter-wavelength mode of Strip 3. The dual-resonance mode shifts to lower frequencies with an increase in the width t [see Fig. 7(b)]. To cover the desired 704 ~ 960 MHz band, the width t is chosen to be 3 mm in the proposed antenna. Also note that for both cases in Figure 7, relatively small effects on the upper band are seen. Over the desired 1710 ~ 2690 MHz band, the impedance matching is all better than 6-dB return loss for all the curves shown.

Figure 8 shows the simulated return loss as a function of the end-section length b of Strip 2. Results for the length b varied from 11 to 17 mm are shown. In this case, very small effects on the lower band are seen. On the contrary, significant effects on the impedance matching of the upper band are observed. This behavior is largely because the length b controls the excitation of the 2.2-GHz band and also affects the impedance matching of the 1.7-GHz mode contributed by Strip 3 as shown in Figure 4. Hence, a proper selection of the length b is important in leading to good impedance matching of the desired upper band of the antenna. The preferred length b is 17 mm in this study. From the above discussion, it can be concluded that the two-branch strip as a coupling feed in the proposed antenna shows different coupling effects as compared with those of the coupling feed in the traditional coupled-fed shorted monopole or planar-inverted-F antennas (PIFAs) [28–33] in which the traditional coupling feed does not contribute additional resonant modes to help enhance the operating bandwidth of the antenna.

Figure 9 shows the simulated return loss for the proposed antenna with and without a USB connector placed nearby. Two cases of the USB connector (size $9 \times 7 \times 4$ mm³ [17, 18]) modeled as a conducting box in very close proximity to the antenna are studied. The first case is the USB connector mounted on the front surface of the main circuit board and in close proximity to the antenna. The USB connector is also grounded through a via-hole to the system ground plane on the back surface of the main circuit board. The second case is the USB connector mounted on the back surface of the main circuit board and flushed to the boundary of the no-ground portion on which the antenna is surface-mounted. From the results, it is

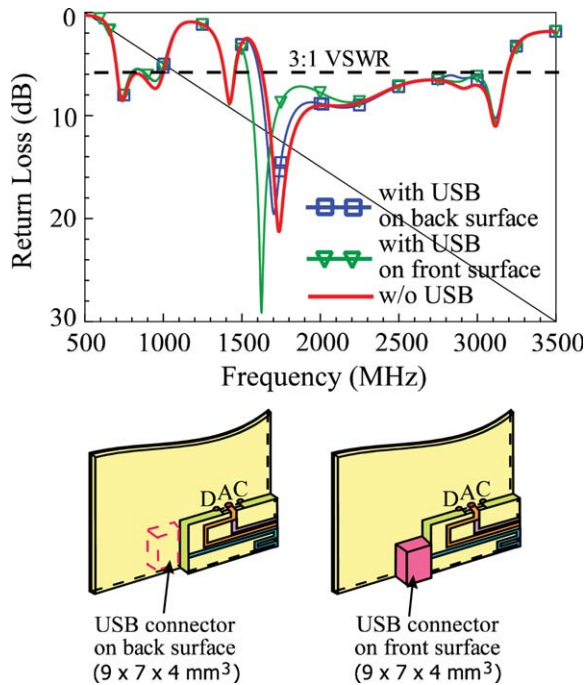


Figure 9 Simulated return loss for the proposed antenna with and without a USB connector modeled as a metallic box and placed in very close proximity to the antenna. [Color figure can be viewed in the online issue, which is available at wileyonlinelibrary.com]

seen that there are small effects on the impedance matching of the antenna. This suggests that the proposed chip antenna is promising to be closely integrated with nearby conducting elements or electronic elements in the mobile handset for practical applications.

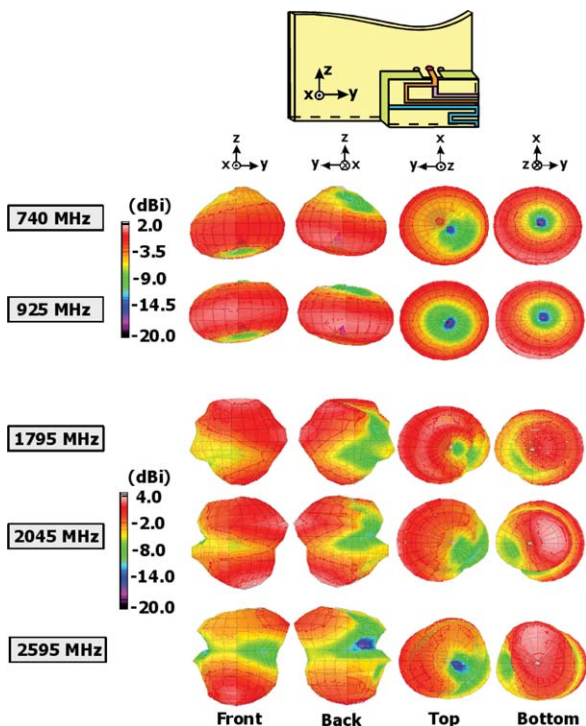


Figure 10 Measured three-dimensional total-power radiation patterns for the fabricated antenna. [Color figure can be viewed in the online issue, which is available at wileyonlinelibrary.com]

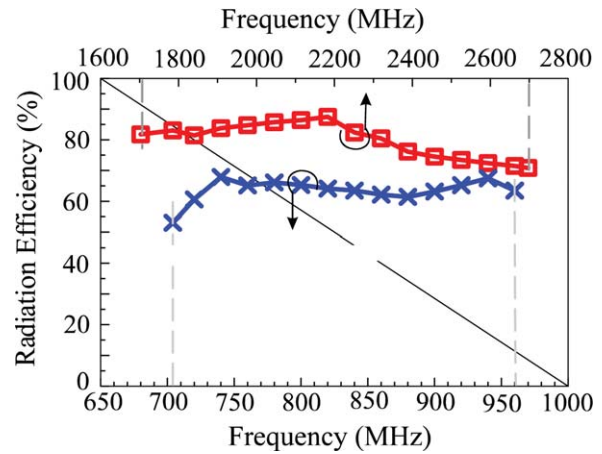
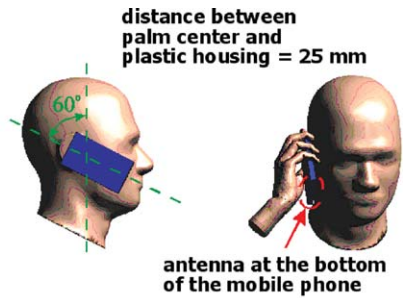


Figure 11 Measured antenna efficiency (mismatching loss included) for the fabricated antenna. [Color figure can be viewed in the online issue, which is available at wileyonlinelibrary.com]

The radiation characteristics of the fabricated antenna shown in Figure 2 are also measured. Figure 10 shows the measured three-dimensional total-power radiation patterns for the antenna. At each frequency, four radiation patterns seen in the front, back, top and bottom directions are shown. For lower frequencies at 740 and 925 MHz, the radiation patterns are close to those of the half-wavelength dipole antenna, and omnidirectional radiation is seen in the azimuthal plane (x - y plane) of the mobile handset. For higher frequencies at 1795, 2045, and 2595 MHz, the obtained radiation patterns show some dips or nulls in the azimuthal plane, and the patterns are close to those of the dipole antenna at its higher-order resonant modes. The obtained radiation patterns are similar to those of the internal WWAN/LTE mobile handset antennas that have been reported [1–8]. This behavior again confirms that the system ground plane of the mobile handset, which is also an efficient radiator, strongly affects and dominates the radiation patterns of the internal handset antenna.

Figure 11 shows the measured antenna efficiency for the fabricated antenna. The measured antenna efficiency includes the mismatching loss. Over the lower and upper bands, the antenna efficiency is respectively about 52 ~ 66% and 70 ~ 86%, which are all better than 50% and acceptable for practical handset applications.

The SAR results for the proposed antenna are also analyzed. Figure 12 shows the SAR simulation model provided by SEM-CAD X version 14 [34], and the simulated SAR values for 1-g tissue at the central frequencies of the eight operating bands. Two cases of the head only and the head and hand are analyzed. The grip of the user's hand on the mobile handset is shown in the figure, with the distance between the palm center and the plastic housing of the handset chosen to be 25 mm. Note that the antenna is mounted at one corner of the bottom edge of the main circuit board. The input power for the SAR testing is 24 dBm at 859 and 925 MHz for the GSM850/900 operation and 21 dBm at 1795, 1920, and 2045 MHz for the GSM1800/1900/UMTS operation. At 740, 2350, and 2595 MHz for the LTE700/2300/2500 operation, the input power is also set to 21 dBm for the SAR testing. The return loss at each frequency for the head only and the head and hand is also shown in the figure. The results indicate that the variations in the return loss are small when the user's hand is added in the SAR testing. The obtained 1-g SAR results for the case of head only are well below the limit of 1.6 W/kg [24]. For the case of head and hand, the SAR values are in general increased, especially at higher frequencies.



Frequency (MHz)		740	859	925	1795	1920	2045	2350	2595
1-g SAR (W/kg)	head only	0.24	0.64	0.64	0.49	0.46	0.39	0.35	0.51
	head and hand	0.37	0.68	0.64	1.15	0.98	0.81	0.95	1.67
Return loss (dB)	head only	10.6	9.2	11.4	10.0	8.0	8.5	7.6	5.8
	head and hand	11.5	8.7	10.2	11.4	8.2	7.8	7.1	6.5

Figure 12 SAR simulation model and the simulated SAR values for 1-g tissue. [Color figure can be viewed in the online issue, which is available at wileyonlinelibrary.com]

This behavior may be related to the smaller wavelengths at higher frequencies, which become comparable to the dimensions of the fingers of the hand phantom. At 2595 MHz, the SAR value reaches 1.67 W/kg, much higher than that (0.51 W/kg) of the head only and also higher than the limit of 1.6 W/kg. When the user's hand is required in the SAR testing in the future, the higher SAR value at higher frequencies needs to be considered in practical handset applications. For other frequencies, the SAR values for the head and hand are still less than 1.6 W/kg.

4. CONCLUSIONS

An internal handset wideband chip antenna with a small size of $3 \times 15 \times 35 \text{ mm}^3$ (about 1.6 cm^3) for eight-band WWAN/LTE operation and capable of close integration with nearby conducting or electronic elements has been proposed. Wideband operation of the antenna is obtained by using a two-branch strip as an efficient radiator and also as a coupling feed to capacitively excite a shorted strip. Close integration of the antenna with nearby conducting elements is achieved by adding ground planes on two side surfaces of the antenna, which are to be grounded to the system ground plane of the handset. Results showing wideband operation and close integration with nearby conducting elements for the antenna have been presented and discussed. Good far-field radiation characteristics of the antenna have been observed. The SAR results which are associated with the near-field emission of the antenna have also been studied. The obtained SAR values for the 1-g head tissue over the eight operating bands are well less than 1.6 W/kg, making the antenna promising for practical applications. When the user's hand is added in the SAR evaluation, although the 1-g SAR values are quickly increased at higher frequencies, it is still promising for the proposed antenna to meet the limit of 1.6 W/kg, because in practical handsets some electronic elements are usually very lossy, which will result in lower SAR values than those obtained in this study.

REFERENCES

1. F.H. Chu and K.L. Wong, Simple planar printed strip monopole with a closely-coupled parasitic shorted strip for eight-band LTE/GSM/UMTS mobile phone, *IEEE Trans Antennas Propag* 58 (2010), 3426–3431.

2. C.T. Lee and K.L. Wong, Planar monopole with a coupling feed and an inductive shorting strip for LTE/GSM/UMTS operation in the mobile phone, *IEEE Trans Antennas Propag* 58 (2010), 2479–2483.
3. K.L. Wong, M.F. Tu, C.Y. Wu, and W.Y. Li, Small-size coupled-fed printed PIFA for internal eight-band LTE/GSM/UMTS mobile phone antenna, *Microwave Opt Technol Lett* 52 (2010), 2123–2128.
4. S.C. Chen and K.L. Wong, Bandwidth enhancement of coupled-fed on-board printed PIFA using bypass radiating strip for eight-band LTE/GSM/UMTS slim mobile phone, *Microwave Opt Technol Lett* 52 (2010), 2059–2065.
5. K.L. Wong and W.Y. Chen, Small-size printed loop-type antenna integrated with two stacked coupled-fed shorted strip monopoles for eight-band LTE/GSM/UMTS operation in the mobile phone, *Microwave Opt Technol Lett* 52 (2010), 1471–1476.
6. S.C. Chen and K.L. Wong, Small-size 11-band LTE/WWAN/WLAN internal mobile phone antenna, *Microwave Opt Technol Lett* 52 (2010), 2603–2608.
7. K.L. Wong, W.Y. Chen, C.Y. Wu, and W.Y. Li, Small-size internal eight-band LTE/WWAN mobile phone antenna with internal distributed LC matching circuit, *Microwave Opt Technol Lett* 52 (2010), 2244–2250.
8. K.L. Wong and C.T. Lee, Wideband surface-mount chip antenna for eight-band LTE/WWAN slim mobile phone application, *Microwave Opt Technol Lett* 52 (2010), 2554–2560.
9. X. Zhang and A. Zhao, Bandwidth enhancement of multiband handset antennas by opening a slot on mobile chassis, *Microwave Opt Technol Lett* 51 (2009), 1702–1706.
10. R.A. Bhatti, Y.T. Im, and S.O. Park, Compact PIFA for mobile terminals supporting multiple cellular and non-cellular standards, *IEEE Trans Antennas Propag* 57 (2009), 2534–2540.
11. A. Cabedo, J. Anguera, C. Picher, M. Ribo, and C. Puente, Multi-band handset antenna combining a PIFA. Slots, and ground plane modes, *IEEE Trans Antennas Propag* 57 (2009), 2526–2533.
12. H. Rhyu, J. Byun, F.J. Harackiewicz, N.J. Park, K. Jung, D. Kim, N. Kim, T. Kim, and B. Lee, Multi-band hybrid antenna for ultra-thin mobile phone applications, *Electron Lett* 45 (2009), 773–774.
13. C.L. Liu, Y.F. Lin, C.M. Liang, S.C. Pan, and H.M. Chen, Miniature internal penta-band monopole antenna for mobile phones, *IEEE Trans Antennas Propag* 58 (2010), 1008–1011.
14. M.Z. Azad and M. Ali, A miniaturized Hilbert PIFA for dual-band mobile wireless applications, *IEEE Antennas Wireless Propag Lett* 4 (2005), 59–62.
15. H. Park and J. Choi, Design of broad quad-band planar inverted-F antenna for cellular/PCS/UMTS/DMB applications, *Microwave Opt Technol Lett* 47 (2005), 418–421.
16. H.C. Tung, T.F. Huang, C.Y. Lin, S.W. Lu, and F.J. Yang, Shorted monopole dual band antenna for ultra-thin profile slider mobile phone, *IEEE Antennas Propag Soc Int Symp Dig*, Albuquerque, NM, pp. 4693–4696, 2006.
17. Available at: http://en.wikipedia.org/wiki/Universal_Serial_Bus, Wikipedia, the free encyclopedia: Universal Serial Bus (USB).
18. K.L. Wong and C.H. Chang, On-board small-size printed monopole antenna integrated with USB connector for penta-band WWAN mobile phone, *Microwave Opt Technol Lett* 52 (2010), 2523–2527.
19. S.L. Chien, F.R. Hsiao, Y.C. Lin, and K.L. Wong, Planar inverted-F antenna with a hollow shorting cylinder for mobile phone with an embedded camera, *Microwave Opt Technol Lett* 41 (2004), 418–419.
20. C.M. Su, K.L. Wong, C.L. Tang, and S.H. Yeh, EMC internal patch antenna for UMTS operation in a mobile device, *IEEE Trans Antennas Propag* 53 (2005), 3836–3839.
21. K.L. Wong and C.H. Chang, Surface-mountable EMC monopole chip antenna for WLAN operation, *IEEE Trans Antennas Propag* 54 (2006), 1100–1104.
22. K.L. Wong and C.H. Chang, An EMC foam-base chip antenna for WLAN operation, *Microwave Opt Technol Lett* 47 (2005), 80–82.
23. C.M. Su, K.L. Wong, B. Chen, and S. Yang, EMC internal patch antenna integrated with a U-shaped shielding metal case for mobile device application, *Microwave Opt Technol Lett* 48 (2006), 1157–1161.

24. American National Standards Institute (ANSI), Safety levels with respect to human exposure to radio-frequency electromagnetic field, 3 kHz to 300 GHz, American National Standards Institute/Institute of Electrical and Electronics Engineers (ANSI/IEEE) standard C95.1, Boulder, CO, 1999.
25. C.H. Li, E. Ofli, N. Chavannes, and N. Kuster, Effects of hand phantom on mobile phone antenna performance, *IEEE Trans Antennas Propag* 57 (2009), 2763–2770.
26. C.H. Chang and K.L. Wong, Printed $\lambda/8$ -PIFA for penta-band WWAN operation in the mobile phone, *IEEE Trans Antennas Propag* 57 (2009), 1373–1381.
27. Available at: <http://www.ansoft.com/products/hf/hfss/>, Ansoft Corporation HFSS.
28. K.L. Wong and C.H. Huang, Bandwidth-enhanced internal PIFA with a coupling feed for quad-band operation in the mobile phone, *Microwave Opt Technol Lett* 50 (2008), 683–687.
29. K.L. Wong and C.H. Huang, Printed PIFA with a coplanar coupling feed for penta-band operation in the mobile phone, *Microwave Opt Technol Lett* 50 (2008), 3181–3186.
30. C.H. Chang and K.L. Wong, Internal coupled-fed shorted monopole antenna for GSM850/900/1800/1900/UMTS operation in the laptop computer, *IEEE Trans Antennas Propag* 56 (2008), 3600–3604.
31. K.L. Wong and S.J. Liao, Uniplanar coupled-fed printed PIFA for WWAN operation in the laptop computer, *Microwave Opt Technol Lett* 51(2009), 549–554.
32. C.H. Chang, K.L. Wong, and J.S. Row, Coupled-fed small-size PIFA for penta-band folder-type mobile phone application, *Microwave Opt Technol Lett* 51 (2009), 18–23.
33. C.T. Lee and K.L. Wong, Uniplanar coupled-fed printed PIFA for WWAN/WLAN operation in the mobile phone, *Microwave Opt Technol Lett* 51 (2009), 1250–1257.
34. Available at: <http://www.semcad.com>, SEMCAD, Schmid & Partner Engineering AG (SPEAG).

© 2011 Wiley Periodicals, Inc.

DESIGN AND DEVELOPMENT OF FLEXIBLE FABRIC ANTENNA FOR BODY-WORN APPLICATIONS AND ITS PERFORMANCE STUDY UNDER FLAT AND BENT POSITIONS

Sankaralingam Subramaniam and Bhaskar Gupta

Department of Electronics and Telecommunication Engineering, Jadavpur University, Kolkata 700 032, West Bengal, INDIA; Corresponding author: slingam.nec@gmail.com

Received 6 December 2010

ABSTRACT: *Modern communication systems are driven by the concept of being connected anywhere and at any time. Fuelled by the idea of a body-centric approach to modern communication technology, many research projects have been initiated to integrate antennas and radio frequency (RF) systems into clothes with regard to size reduction and cost-effectiveness; so that the wearer may not notice the existence of these subsystems. For instance, the development of wearable computer systems has been very rapid and soon one will see a wide range of unobtrusive wearable and ubiquitous computing equipment into his/her everyday wear. Rapid progress in wireless communication promises to replace all wired-communication networks in the near future, in which antennas play a vital role. This paper describes design and development of a circular patch antenna for on-body wireless communications. This antenna makes use of polyester-combined cotton [65:35] fabric as its dielectric material and the conducting parts of the antenna are made up of copper. The impedance and radiation characteristics are determined experimentally when the antenna is kept in flat position. The performance characteristics of the antenna are analyzed under bent conditions too, to check compatibility with wearable applications.*

Results demonstrate the suitability of this kind of patch antenna for on-body wireless communications. © 2011 Wiley Periodicals, Inc. *Microwave Opt Technol Lett* 53:2004–2011, 2011; View this article online at wileyonlinelibrary.com. DOI 10.1002/mop.26188

Key words: *fabric substrate; circular disk microstrip wearable antenna; impedance and radiation characteristics*

1. INTRODUCTION

Communications on the human body is a relatively unexplored domain for the personal and mobile communications community. Perhaps, only the military and the special services, such as firefighters, have been using so far on-body systems [1] to support their users in various hazardous environments. A wearable antenna is considered as an essential component in body-centered wireless local area networks (LANs) and, therefore, it plays a significant role in optimal design of any wearable system. For the wireless body-centric network to be accepted by the public, wearable antennas need to be hidden and of low profile. This requires a possible integration of these systems within everyday clothing. Microstrip patch is a suitable candidate for any wearable application, as it can be made conformal for integration into clothing [2–4]. Till date most of the research effort is put for rectangular-shaped patch antennas intended for such wearable applications [5–7]. A rectangular patch with truncated corners has been discussed in [8]. Reference 9 has described a dual-band coplanar patch antenna integrated with an electromagnetic band gap substrate. A rectangular ring microstrip patch is presented in [10].

The aim of this article is to design, develop, and evaluate the performance characteristics of body-centric microstrip Bluetooth antennas with circular geometry, meeting the IEEE 802.11(b) standards. The fabrication process involved in the work reported here is substantially simple and easily compared to that involved in designs reported in [7–10]. This antenna makes use of polyester-combined cotton [65:35] fabric as its dielectric material and its conducting parts are made up of copper. The simulated and experimental results on impedance and radiation characteristics of this wearable antenna are presented when it is kept in flat position. However, in the case of on-body environment, it is difficult to keep the wearable antenna flat all the time, and it becomes bent frequently due to body movements. The bending may modify the performance characteristics of the antenna as its radius gets altered. Hence, an experimental study is to be carried out to investigate the effects of antenna bending on its performance characteristics such as resonant frequency, return loss, impedance bandwidth, gain, and radiation patterns. In [7], the author has used rectangular patch in an array environment. The bending effect was analyzed for only one value of radius of curvature (146 mm). In [8], the author has used square patch with truncated corners, and the patch was analyzed with bending radius of 40 mm. Reference [9] has described a dual-band coplanar waveguide (CPW)-fed coplanar antenna for wearable application, and the structure was bent for analysis with radii of 40 and 70 mm. In [10], a rectangular ring antenna has been discussed with bending radii of 60 and 37.5 mm.

In this article, the authors have used circular geometry, and the investigation on bending effects is more exhaustive in the sense of covering higher range of bending (with radii of 50.8, 63.5, 76.2, and 88.9 mm). For at least three cases (bending radii of 88.9 and 76.2 mm and flat position), the designs are found to be robust and to cover the Instrument, Scientific, and Measurement (ISM) band. The rest of the article has been organized as follows: Section 2 discusses design aspects, modeling, and fabrication of antenna. Both simulated and measured results on performance characteristics of flat antennas under investigation are